THERMAL ANALYSIS OF A SOLAR CONCENTRATING COLLECTOR WITH NONUNIFORM FLUX DISTRIBUTION

H.E. Gad, H.A. El-Seddiek and M.M. Awad

Mechanical Power Department, Faculty of Engineering
Mansoura University

التحليل الحرارى لمركز شمسى مع وجود فيض اشعاعى غير منظم

خلاصة - يستعرض هذا البحث استخدام طريقة سريان الاشارة البيانية فى التحليل الحرارى لمركز شمسى مسطح ومعرض لفيض اشعاعى غير منتظم ، حيث يتم تمثيل جميع متغيرات النظام والعلاقات بينها (كاشارات لها قيم معلومة) فى تركيب بيانى مبسط ، ويمكن ايجاد قيمة أى متغير مباشرة باستخدام خواص هذا التركيب البيانى . وتتميز هذه الطريقة بعدم ضرورة فرض انتظام الفيض كما هو الحال عند التحليل بطريقة هوتيل - وبلير - ورتز - بلس ، وقد تم عمل برنامج كمبيوتر لايجاد نتائج التحليل الحرارى بالطريقتين تحت ظروف مختلفة ومقارنتها بالنتائج العملية . ولهذا الغرض تم انشاء جهاز تجريبى عبارة عن مركز شمسى يتكون سطحه الداكن من قطع مرايا غير متساوية ومرتبة بطريقة معينة لتركيز معظم الاشعاع الساقط على الثلث العلوى للمستقبل طوله ٩٤ سم وعرضه ٢٥ سم ومصمم بحيث يكون سريان الماء بداخله شبه منتظم ومعزول بالصواج فوم سمكها ٣ سم ومثبت داخل صندوق خشبى يمكن وضع غطاء زجاجى عليه . وقد أعد الجهاز لقياس توزيع درجات الحرارة فى أماكنه المختلفة وشدة الاشعاع الشمسى المباشر العمودى والكلى الافقى ودرجة حرارة الهواء ومعدل سريان الماء أثناء التجارب العملية . وقد اظهرت المقارنة بين النتائج النظرية والعملية تطابقا أكثر فى حالة استخدام طريقة سريان الاشارة البيانية ويعتبر ذلك مؤشرا مشجعا لامكانية الاعتماد عليها للحصول على نتائج دقيقة للتحليل الحرارى للمستقبل فى مركزات الطاقة الشمسية .

ABSTRACT- This paper presents a new approach to the thermal analysis of a solar concentrator. The Signal Flow Graph technique is applied to solve the heat transfer problem in a flat receiver subjected to nonuniform flux distribution. Signal Flow Graph allows in a more easy graphical form to express the essential properties of the analyzed system, and directly obtain any parameter from the graph structural properties. With this method, there is no need of assuming uniform flux distribution over the whole receiver surface as in Hottel-Whillier-Woertz-Bliss approach. A computer program has been established to obtain the thermal performance under different design and operating conditions using both approaches. In order to verify the theoretical results, an experimental concentrator was built with, one glass cover, flat receiver of 25 cm width and 94 cm length. The receiver is insulated with foam plates of 3 cm thickness and fitted with two headers to supply the fresh water uniformly in the length direction. The reflecting surface is formed of unequal mirror segments which are arranged to concentrate most of the falling solar radiation on the upper third of the receiver surface. The set-up is suitably instrumented to measure the temperature at different points and the water mass flow rate through the receiver. The total and beam solar radiation intensities as well as the ambient temperature are also measured during the experimental work. Comparison between the predicted and measured

results have shown that the thermal performance as calculated by the Signal Flow Graph is more fitted with the experimental results than that obtained by the HWWB approach. Therefore, the Signal Flow Graph approach is seen to be an easy and precise technique for the thermal analysis of concentrating collectors with nonuniform flux distribution on the receiver surface.

INTRODUCTION

The thermal analysis of solar concentrators is essentially required to improve the collection efficiency and hence reduce their production cost for commercial use. Normally, the solar flux distribution over a receiver surface of any concentrating collector has a degree of nonuniformity, which complicates their thermal analysis. However, most of the reported data on the thermal analysis of solar concentrators are still based on the well known Hottel-Whillier-Woertz-Bless (HWWB) approach (1-3), by which the thermal performance could be calculated. The solution of thermal performance by this approach is usually simplified by assuming the flux to be uniformly distributed over the receiver surface (4-7). On the other hand, the temperature field in solar receivers could be obtained by the solution of energy equations as reported by Cabble (8). Again, he has considered the same assumption to simplify his theoretical analysis. However, a considerable error may result due to this assumption specially when the temperature field is to be calculated.

However, the exact solution of the problem with nonuniform flux distribution is essentially required in order to obtain precise results for the temperature field of the system. Signal Flow Graph Technique, which is usually used in the solution of control linear systems, offers this facility. This technique can be used also to obtain the temperature field in thermal systems (9-10). In the present work, this technique is used for the first time, according to the authers knowledge, in the thermal analysis of solar concentrators. The main advantage of the Signal Flow Graph is that the heat transfer problem, with all variables involved, can be expressed in an easy graphical language to get the exact solution in minimum time.

THEORETICAL MODEL

It is required to calculate the temperature field for a flat receiver of width R, and length L. The receiver is subjected to a flux distribution in the width direction as shown in Fig. 1. The flux changes with time in both width and length directions. The following assumptions are made to simplify the solution,

i - Steady state condition,
ii - The flux change in length direction is neglected,
iii - The fluid flow rate change in length direction is neglected.

With the above situation, the problem is reduced to a two dimensional heat transfer in both width and perpendicular directions. Conduction heat transfer in the absorber plate is carried out in the width direction. On the other hand, the useful convection heat from the plate to fluid, and the heat losses to the ambient (convection and radiation) are perpendicular to the absorber plate. These modes of heat transfer can be formulated by means of Signal Flow Graph as given below.

Signal Flow Graph is a graphical representation of the relations between all parameters in any linear system. These parameters can be easily expressed and directly obtained from the graph structural properties of the system. To solve this problem by the Signal Flow Graph, the receiver should be divided into a number of slices N, in the width direction, such that the flux may be considered uniform over each one and equal to the corresponding average value as shown in Fig .1. The temperature field for a receiver divided into 5 slices could be represented by a Signal Flow Graph as shown in Fig. 2. The

graph consists of two types of nods connected with branches, transmittance of which carry signals from one node to the other. The source nodes don't have feed-back signals, (i.e. independent variables) such as the inlet water temperature T_i, ambient temperature T_a, and the solar energy absorbed by each slice Q_i. The sink nodes must have feed-back signals (i.e. dependent variables). All the unkown plate temperatures T_{p1}, T_{p2}, . . ., T_{p5} and the fluid temperatures T_{f1}, T_{f2}, . . ., are the sink nodes.

The physical value of any branch transmittance S_{ij} from nod i to another j can be obtained by the help of heat balance equation for the node j. As an example, the heat balance equation for the node 2 on the absorber plate yields,

$$C_p (T_{p1} - T_{p2}) + C_p(T_{p3} - T_{p2}) + C_{f2}(T_{f2} - T_{p2}) + C_{cp2}(T_c - T_{p2}) + Q_2 = 0 \quad \ldots (1)$$

where,

C_p is the plate material thermal conductance,

C_{f2} is the thermal conductance between the fluid and plate at node 2,

C_{cp2} is the thermal conductance between the cover and plate at node 2 (by convection and radiation), and

Q_2 is the solar energy absorbed by the slice 2.

However, equation 1 could be rearranged to give the signal value at node 2 (T_{p2}) as,

$$T_{p2} = S_{12}\, T_{p1} + S_{32}\, T_{p3} + S_{72}\, T_{f2} + S_{c2}\, T_c + S_{q2}\, Q_2 \quad \ldots (2)$$

Generally, S_{ij} can be evaluated from,

$$S_{ij} = C_{ij} / C_j \quad \ldots (3)$$

where, C_{ij} is the thermal conductance between nodes i and j

and C_j is the sum of all thermal conductances from all adjacent nodes to the node j.

It is to be noted that $C_{ij} = 1$ when i refers to the absorbed solar energy source node (i.e $S_{qj} = 1 / C_j$).

For the node 2,

$$C_2 = 2\, C_p + C_{f2} + C_{cp2} \quad \ldots (4)$$

Equation 2 shows that the signal value at any node can be expressed as the sum of products of all signal values of the adjacent nodes by the corresponding branches transmittance which enter the node. On the other hand, equation 3 shows that the value of branches transmittance can be obtained without the solution of heat balance equations at different nodes.

In the present work, the different thermal conductances are calculated as follows:

a- Thermal conductance through back insulation C_b, is constant for all slices and is given by,

$$C_b = (K / D)\, A_s \quad \ldots (5)$$

where, K is the thermal conductivity of the insulating material
D is the insulation thickness
and A_s is the slice area = (R/N) L

b- Thermal conductance between plate slices C_p, is also constant and is given by,

$$C_p = (K_p\ N/R)\ (L\ d) \qquad \ldots (6)$$

where, K_p is the plate material thermal conductivity,
and d is the plate thickness

c- Thermal conductance between fluid slices C_f, is given by,

$$C_f = c\dot{m} \qquad \ldots (7)$$

where, c is the fluid specific heat which is assumed constant in the given temperature range,
and $\dot{m}$ is the fluid flow rate.

d- Thermal conductance between the fluid and plate C_{fj}, is given by

$$C_{fj} = h_f\ A_s \qquad \ldots (8)$$

where, h_f is the film heat transfer coefficient between the fluid and plate which is calculated from (11) as,

$$Nu = 0.199\ Re^{0.32} Pr^{0.33} (Gr \cdot Pr)^{0.1}\ (Pr / Prw)^{0.25}\ \lambda$$

where λ is a factor depending on the aspect ratio, (R / L).
Since h_f is a temperature dependent, then C_{fj} value changes with the slice position.

e- Thermal conductance between the cover and plate C_{cpj} is given by,

$$C_{cpj} = \left[h_c + \frac{(T_p^2 + T_c^2)(T_p + T_c)}{1/\epsilon_p + 1/\epsilon_c - 1} \right] A_s \qquad \ldots (9)$$

where h_c is the convection heat transfer coefficient calculated from (12) as,

$$Nu = 0.033\ (Gr)^{0.381}$$

Again, C_{cj} is temperature dependent.

f- Thermal conductance between the cover and air C_{ca} , is given by

$$C_{ca} = \left[h_w + \frac{6\epsilon_p (T_p^4 - T_s^4)}{T_p - T_s} \right] A_s \qquad \ldots (10)$$

where , h_w is the wind heat transfer coefficient calculated from (13) as,

$$h_w = 5.7 + 3.8\ V_w \qquad (\ W/m^2\ ^\circ C)$$

where, V_w is the wind speed (m/s).

Now, any sink node value (i.e any required temperature in the field) can be directly obtained from Mason's formula (13) as,

$$\text{Sink node value} = \sum_{j=1}^{n_s} (\text{source})_j\ (TR)_j \qquad \ldots (11)$$

where, n_s is the number of sources in the system, and, $(TR)_j$ is the transmittance from the source j to the node given by,

$$(TR)_j = \sum_{k=1}^{n_p} P_k \Delta_k / \Delta \quad \ldots (12)$$

where, n_p is the number of pathes from the source to sink node,

P_k is thepath transmittance which is equal to the product of all its branches transmittance,

Δ is the graph determinant,

and, Δ_k is the algebric supplement of the path which is equal to the graph determinant in which all loops that touch the path are equal to zero.

However, if L_p is the loop transmittance which is defined by the product of branches transmittance of a closed loop in the graph, then,

$$\Delta = 1 - (\sum_{i=1}^{\Theta} L_{p_i}) + (L_{p1} L_{p2} + L_{p2} L_{p3} + \ldots) - (L_{p1} L_{p2} L_{p3} + \ldots) \quad \ldots (13)$$

where, Θ is the number of closed loops in the graph, and all terms between the last two parentheses are concerned with all the nontouching loops.

Once the temperature field is determined from the above equations, the rate of useful heat gain Q_u, can be calculated from,

$$Q_u = \sum_{j=1}^{N} [\, C_{fj} (T_{pj} - T_{fj}) - C_b (T_{fj} - T_a) \,] \quad \ldots (14)$$

and the collector thermal efficiency η_c, is given by,

$$\eta_c = Q_u / I_{ta} \, NA_s \quad \ldots (15)$$

while the fluid outlet temperature T_o, can be calculated from,

$$T_o = T_i + Q_u / c \dot{m} \quad \ldots (16)$$

A computer program has been established to perform the above calculations, half an hour intervals, during the sunshine period by iterative method. This is carried out by assuming a temperature field and then recalculated and compared. The error is limited within a range of 0.1 °C.

EXPERIMENTAL SETUP AND PROCEDURE

A multi-mirror asymmetrical concentrator with a flat receiver has been designed and fabricated to verify the predicted results. The reflector surface is formed by 19 unequal width mirror segments, which are arranged such that most of the incident beam radiation is concentrated over the upper third of the receiver surface at noon time. This flux distribution, which changes with time, is obtained by fixing the optical axis of concentrator

twards the sun at noon position. The receiver, which is fixed at the lower edge of reflector, consists of an absorber inside a wooden box and covered with an ordinary window glass cover of thickness 3 mm. Foam plates of thickness 3 cm are used for back insulation. The absorber is made from 0.8 mm thick G.I. sheet and has a width of 25 cm, length Of 94 cm and a distance between plates of 1.5 cm. The upper plate is coated with blackboard paint to increase its absorpitivity to solar radiation to about 0.9 . The absorber headers are designed, with gradually increasing holes from the middle, to maintain a uniform water flow rate in its length direction. The whole assembly is fixed on a wooden frame with a facility to change the concentrator tilt angle.

The setup is suitably instrumented to measure the absorber plate temperature at different locations by copper-constantan thermocouples as shown in Fig.3. The inlet and outlet water temperatures as well as the ambient temperature are also measured. The intensity of normal beam solar radiation is measured by a silicon cell pyrhelionieter, while the horizontal total solar radiation is measured by a silicon cell pyranometer during the experimental work. A Photograph of setup is given at the end of paper.

The experimental tests are carried out in a clear sky condition, during August 1987, by allowing the water to flow from an overhead tank to the receiver. Each day, the flow rate is kept constant. Six tests are conducted with flow rates of 12.75, 9.6 and 6 lit/hr with and without a glass cover on the receiver.

RESULTS AND DISCUSSION

The measured data of beam and total solar radiation intensities, ambient and fresh water temperatures and the actual water mass flow rate are used as input information to obtain the predicted results. In the Signal Flow Graph solution, the predicted flux distribution over the receiver surface, is obtained by the ray tracing technique (14). The average value of this flux distribution is obtained to be used in the solution by HWWP formulation. It was found that dividing the receiver into five slices in our case is a good compromise between the accuracy of results and the computation time. Preliminary experimental tests have shown also that assuming a uniform temperature for the glass cover, will not affect the accuracy of results.

The receiver was experimented first without glass cover, using water mass flow rates of 9.6, 12.75 and 6 lit/hr, in clear sky days. Figure 4.a shows the measured water outlet temperature as a function of time for the three days experimentation. The predicted results obtained with the Signal Flow Graph are also depicted for comparison. On the same figure, the normal beam solar radiation, the horizontal total solar radiation, the fluid inlet and ambient temperatures for an average day are plotted. It can be noted that the fresh water temperature is slightly larger than that of ambient. This is due to the existance of long uninsulated pipe line (with low water flow rate) in the direct sun light. Figure 4.b shows the corresponding temperature rise (T_o - T_i) and the collector thermal efficiency. The following observations can be made from these figures,

a- The outlet temperature increases to a maximum value at noon time and then decreases again.

b- The water temperature rise and hence the collector efficiency are seen to have the same trend.

c- The outlet temperature and hence the temperature rise decrease considerably with the increase of flow rate, while the corresponding change in thermal efficiency is not much. The maximum outlet temperature was decreased from about 91 to 62°C, when the flow rate was increased from 6 to 12.75 lit/hr. The corresponding increase in collector efficiency was from 0.52 to 0.6.

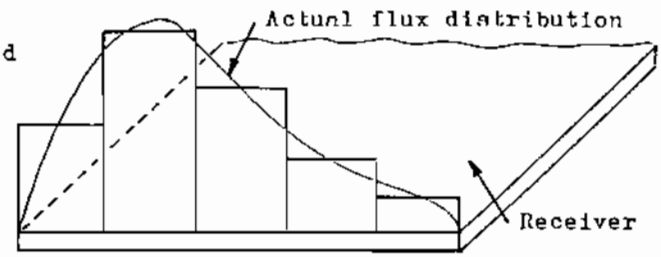

Fig. 1. A receiver divided into five slices.

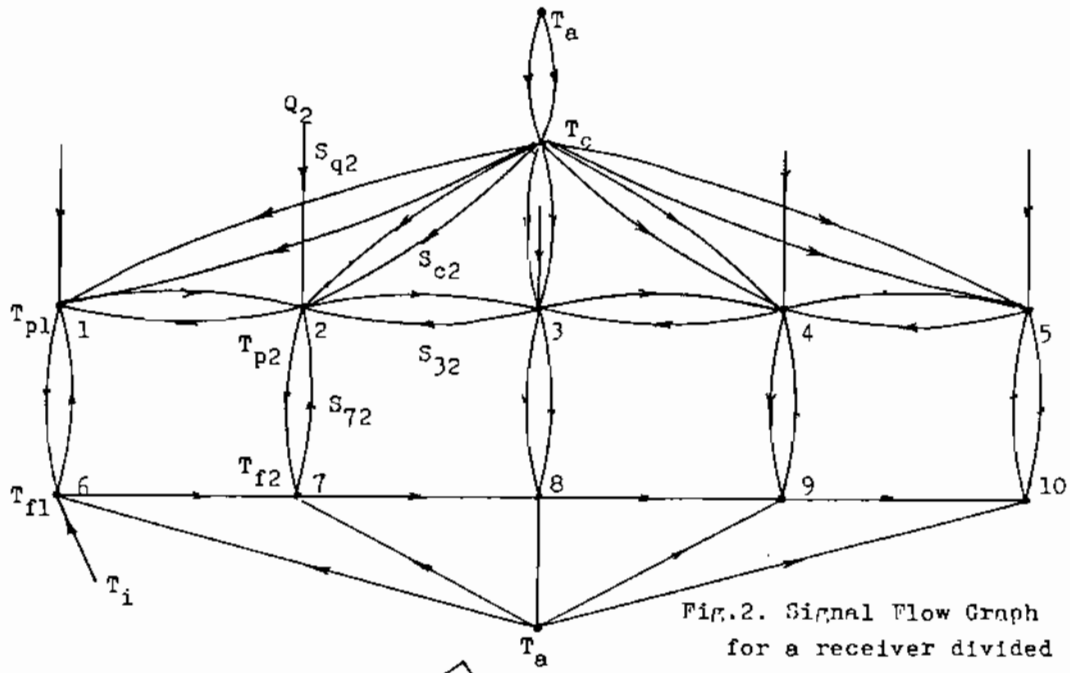

Fig.2. Signal Flow Graph for a receiver divided into five slices.

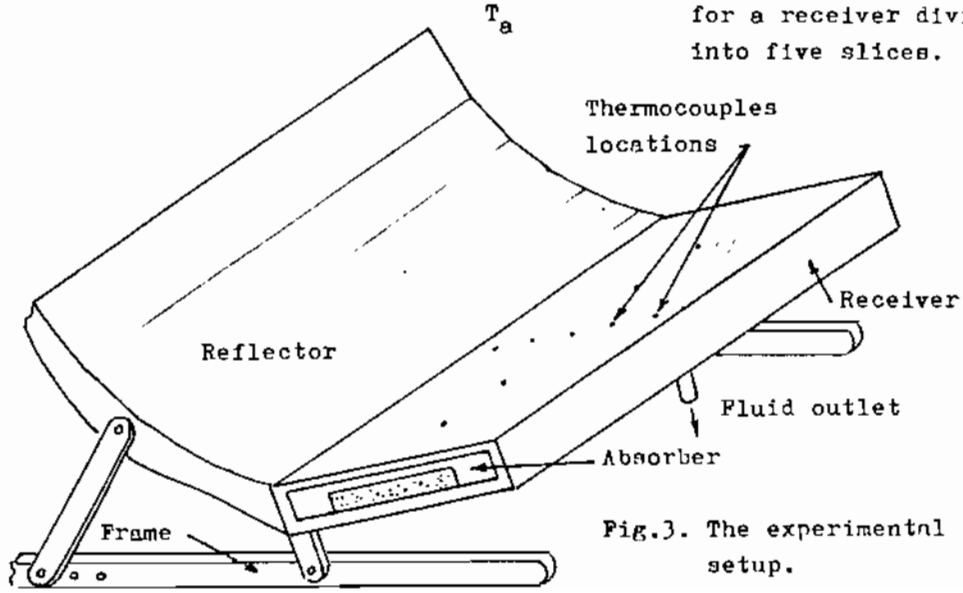

Fig.3. The experimental setup.

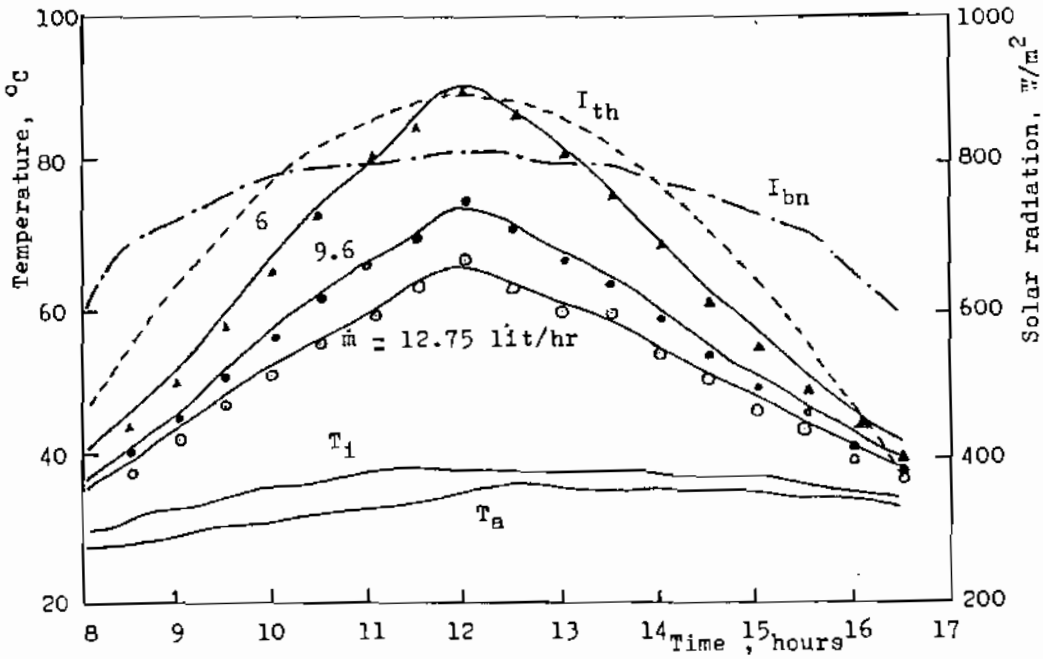

Fig.4a Fluid outlet temperature for the receiver without glass cover

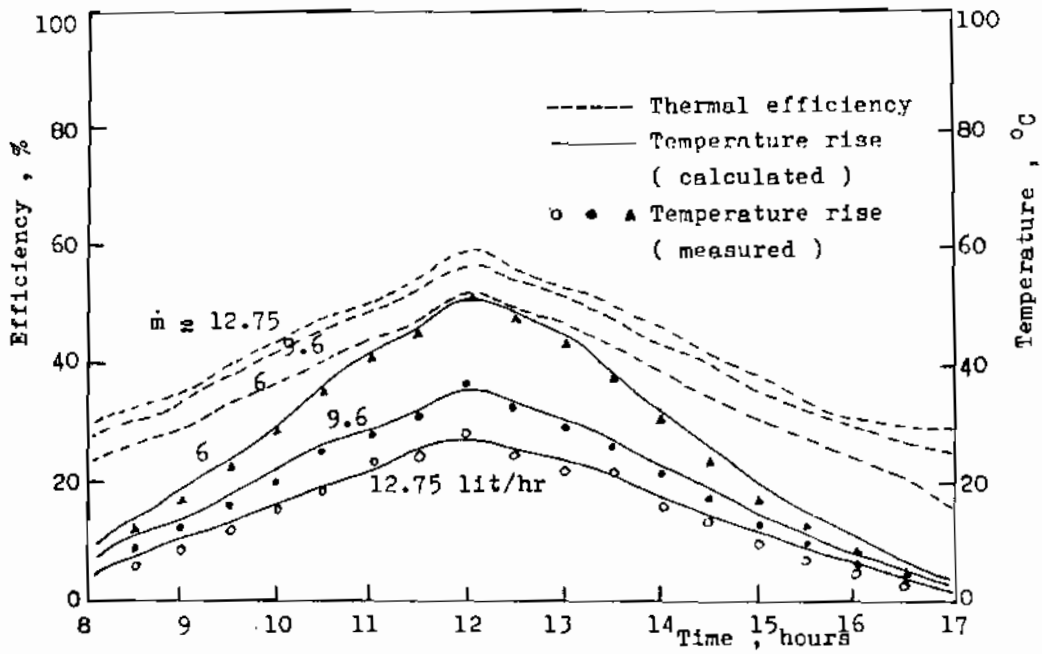

Fig.4b Collector thermal efficiency and fluid temperature rise of the receiver without glass cover.

d- The theoretical results show a very good agreement with the experimental data, specially around the noon time. The slight deviation in the day terminals is due to the increasing optical losses.

The corresponding results with one glass cover on the receiver are shown in Fig. 5. The behaviour of water outlet temperature and the collector thermal efficiency show a similar trend, without any major difference. However, a slight increase in thermal efficiency can be observed, since the maximum temperature rise is not higher than 55°C. The maximum concentration ratio for the concentrator is only 3.64. The effect of flow rate is seen to be slightly depressed due to the existance of the glass cover.

On the other hand, a sample of typical results for the plate temperature distribution in the width direction, measured at the absorber plate centre line is shown in Fig. 6. The calculated plate temperature is plotted at different hours,and compared with the corresponding measured values. The observed drop in the plate temperature near the upper receiver edge at afternoon hours is due to the shift of the flux distribution peak downwards. The good agreement between the theoretical results and experimental data can also be seen.

Finally, a comparison between the theoretical results, obtained by the Signal Flow Graph and HWWB approaches, and the measured data is shown in Fig. 7. The figure shows the fluid outlet temperature as a function of time for the receiver with glass cover, during the three days experimentation. It is clear that the Signal Flow Graph results show a better agreement with experimental results than that obtained by HWWB formulation. This fact would be more visible with different flux distributions for other systems.

CONCLUSIONS

The thermal analysis of solar concentrating collectors with nonuniform flux distribution over the receiver surface can be easily performed with the Signal Flow Graph technique. By this method, all the system parameters and relations between them could be expressed in an easy graphical form to get the exact solution in minimum time. The temperature field in solar receivers, which are subjected to nonuniform flux, can be calculated by using the Signal Flow Graphs to a good exactness, without the need of assuming uniform flux distribution for simplification. The theoretical results obtained by this method have shown a better agreement with the experimental data, collected for a flat receiver under different conditions, than that calculated by HWWB formulation. Therefore, this method is encouraging to obtain solid correlations in thermal analysis with further work on other solar systems.

NOMENCLATURE

A_a	Aperture area, m^2
A_s	Slice area, m^2
C_{ij}	Thermal conductance between nodes i and j, W/ K
C_j	Sum of thermal conductances from all adjacent nodes to j
c	Fluid specific heat, J / kg K
D	Insulation thickness, m
d	Plate thickness, m
Gr	Grashof number
h_c	Convection heat transfer coefficient between the cover and plate, W/m^2 K
h_f	Film heat transfer coefficient between the fluid and plate, W/m^2 K
I_{bn}	Normal beam solar radiation flux, W/m^2

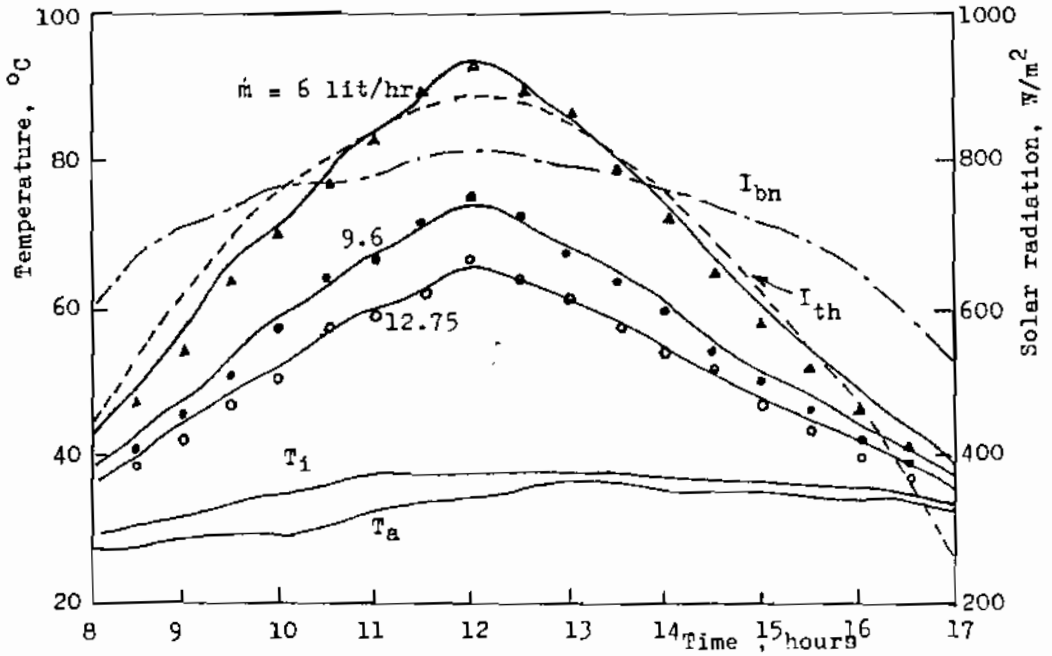

Fig.5a Fluid outlet temperature for the receiver with glass cover.

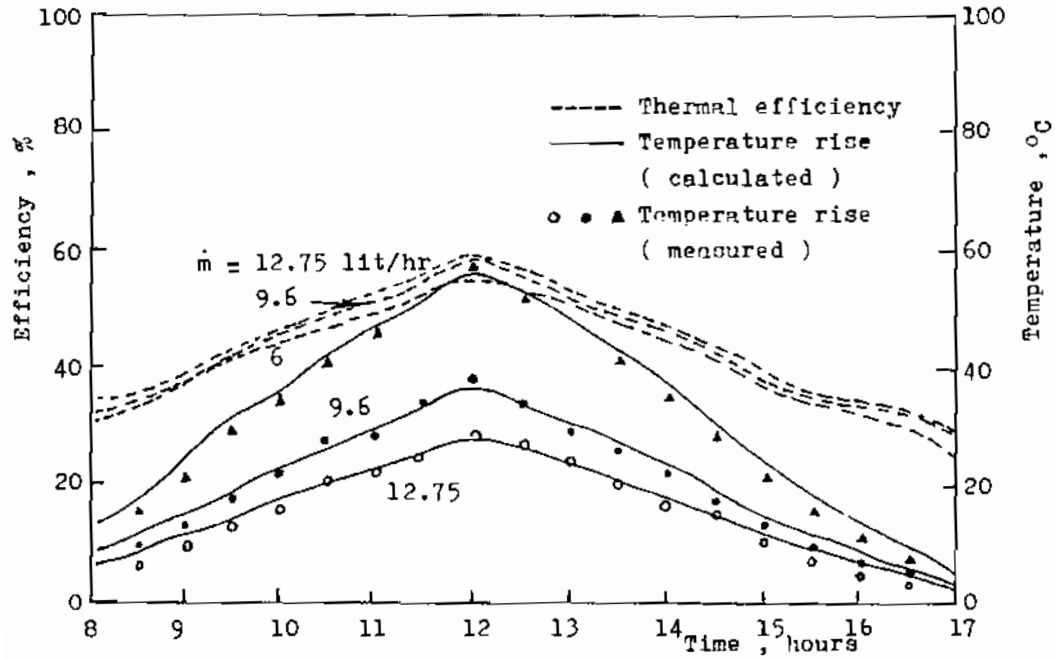

Fig.5b Collector thermal efficiency and fluid temperature rise of the receiver with glass cover.

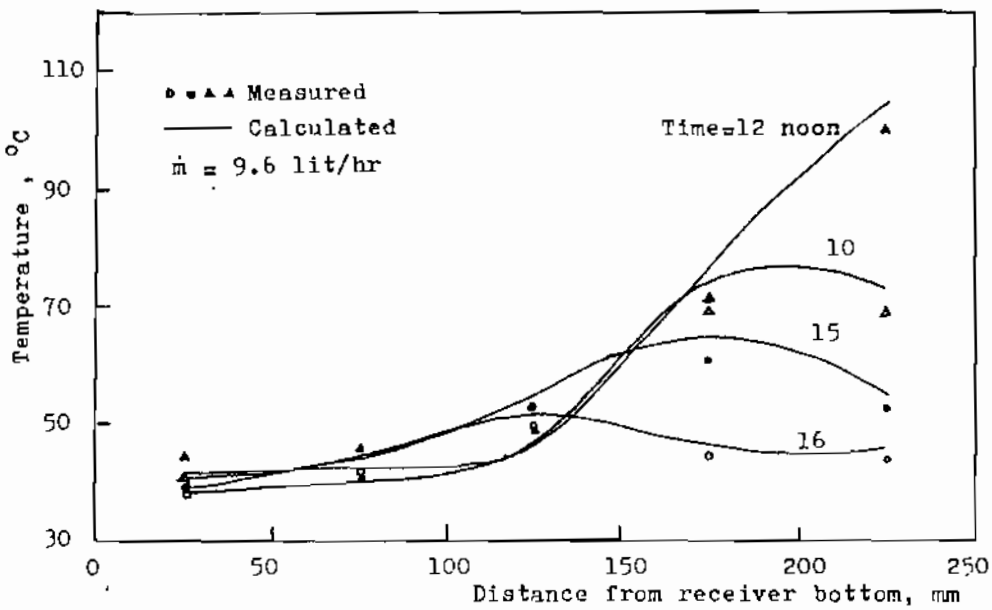

Fig. 6. Plate temperature distribution in the flow direction

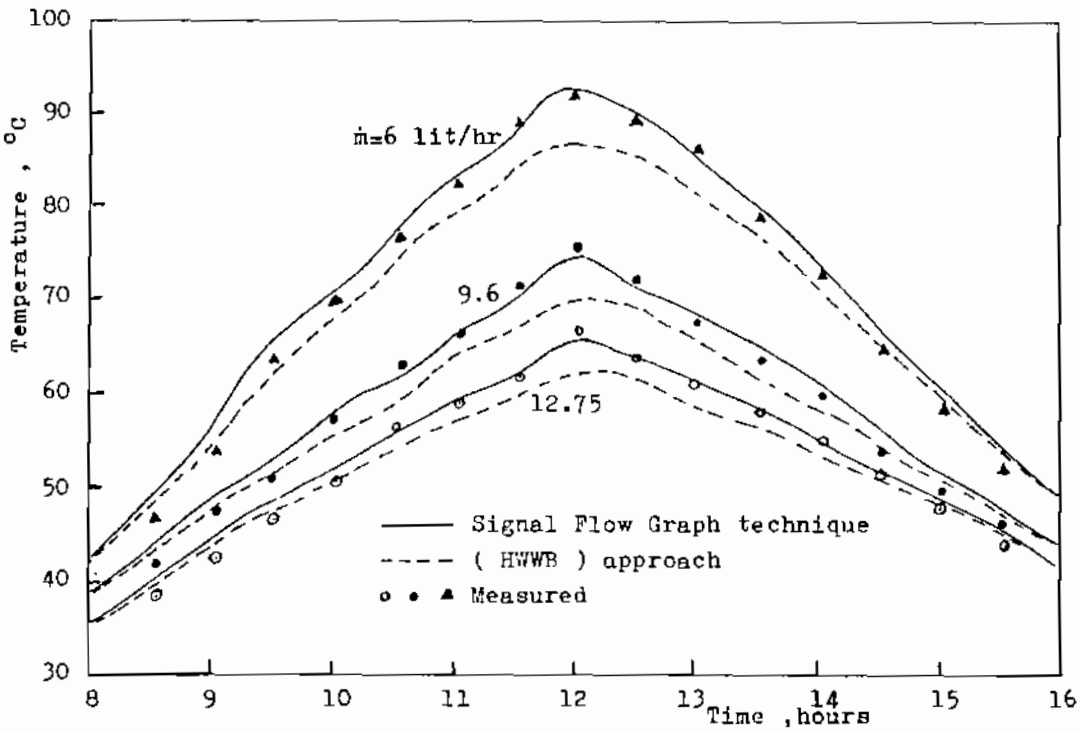

Fig. 7. Comparison between the Signal Flow Graph and HWWB results.

I_{th}	Horizontal total solar radiation flux, W/m²
I_{ta}	Total solar radiation flux on the aperture, W/m²
k	Insulation material thermal conductivity, W/m K
K_p	Plate material thermal conductivity, W/m K
L	Receiver length, m
L_p	Loop transmittance,
$\dot{m}$	Fluid mass flow rate, kg /s
N	Total number of slices
Nu	Nusselt number
n_s	Number of sources
n_p	Number of pathes from the source to sink node
P_k	Path transmittance
Pr	Prandtl number
Prw	Prandtl number calculated at wall temperature
Q_i	Solar energy absorbed by slice number i, W
Q_u	Useful heat gain, W
R	Receiver width, m
S_{ij}	Branch transmittance from node i to j
S_{qj}	Branch transmittance when i is the solar energy source
T	Temperature, °K
T_i	Fluid inlet temperature, °K
T_o	Fluid outlet temperature, °K
T_s	Sky temperature, °K
$(TR)_j$	Transmittance from the source j to a given node
V_w	Wind velocity, m/s

Greek letter symbols

Δ	Graph determinant
Δ_k	Algebric supplement of the path
ϵ_c	Glass cover emissivity
ϵ_p	Plate surface emissivity
η_c	Collector thermal efficiency
Θ	Number of closed loops in the graph
σ	Stefan - Boltzmann constant

Subscripts for thermal condcuctances and temperatures

a	Air
b	Back insulation
c	Glass cover
f	Fluid
i , j	Slice and node number

REFERENCES

1- H.C. Hottle and B.B. Woertz, "Perormance of Flat-Plate Solar Heat Collectors", Trans. ASME, 64,91 (1942).

2- H.C. Hottel and A. Whillier, "Evaluation of Flat-Plate Collector Performance", Trans. Conf. Use Solar Energy 2, 74 (1958).

3- R.W. Bliss, "The Derivation of Several Plate Efficiency Factors Useful in the Design of Flat-Plate Solar Heat Collectors", Solar Energy,3, 55 (1959).

4- A. Rabl, "Optical and Thermal Properties of Compound Parabolic Concentrators", Solar Energy, 18, 497 (1976).

5- R.E. Jones and G.C. Anderson, "Circular Arc Approximations of truncated CPC Collectors", Solar Energy, 25, 139 (1980).

6- C.K. Hsieh, "Thermal Analysis of CPC Collectors", Solar Energy, 27, 19 (1981).

7- L.H.Rabie, M.M. Awad and N.H. Mostafa, "Optical and Thermal Analysis of a Hyperbolic Spiral Solar Concentrator", ISTED Int. Energy Symposia, Cambridge, Mass, 7-9 July (1982).

8- M.H. Cabble, "Heat Exchangers for Solar Concentrators", Solar Energy, Vol.7, No.1, 1963.

9- K.A. Polnitskii and M.M. Awad, "Determination of Temperature Field in the End Part of a Rotor of Cryoturbogenerator by the Help of Graphs", Respoblikanskii Mejvedostveni Naotchnoteknitchiskii Spronik, Issue 24, Kharkov, Vitcha Shkola, (in russian Language), 1977.

10- K.A. Polnitskii and M.M. Awad, "Use of Signal Flow Graphs for the Determination of the Temperature Field in a Stator With Direct Cooling", Elektromekhika, (Jurnal of Electromechanics), (in russian), Moscow, USSR, Vol.1, 1981.

11- V.P. Isachenko, V.A. Osipova and A.S. Sukomel, "Heat Transfer", MIR Publishers, Moscow, Third Edition. Second Printing, 1980.

12- J.A. Duffie and W.A. Beckman, "Solar Energy Thermal Processes", Wiely, New York (1974).

13- K. Ogata, "Modern Control Engineering", Prentice Hall of India Private Limited, New Delhi, 1982.

14- H.E. Gad, H.A. El-Seddiek and M.M. Awad, "The Optical Analysis of an Asymmetrical Piece-Wise Concentrator", Mansoura Engineering Jurnal (MEJ), El-Mansoura University, Vol. 12, No.1, June 1987, PP.M.23-M.33.

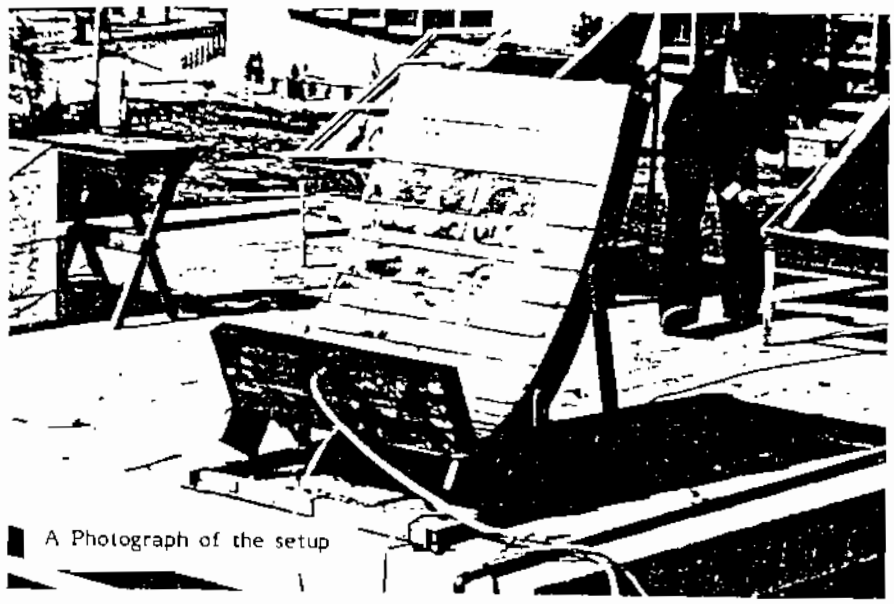

A Photograph of the setup